Improving thermal performance of a ventilated tiled roof by using phase change materials

Michele Bottarelli[1,*], Eleonora Baccega[1], Francisco Javier González Gallero[2], Ismael Rodríguez Maestre[2], Gang Pei[3] and Yuehong Su[4]

[1]Department of Architecture, University of Ferrara, 44122 Ferrara, Italy; [2]Escuela Técnica Superior de Ingeniería de Algeciras, University of Cádiz, 11202 Algeciras, Spain; [3]Department of Thermal Science and Energy Engineering, University of Science and Technology of China, Hefei 230027, China; [4]Department of Architecture and Built Environment, University of Nottingham, Nottingham NG7 2RD, UK

Abstract

The adoption of ventilated roofs and facades, as well as the integration of phase change materials (PCMs) in the building envelope, has proved to be effective as a passive cooling technique in reducing the solar heat gain through the building envelope during the summer period, therefore reducing the energy requirement for cooling. Even though much research focused on each of these strategies individually, their combination has not been deeply studied yet. Preliminary numerical studies were carried out on the application of PCMs on a pitched ventilated tiled roof, and the most effective position turned out to be the one suspended in the middle of the above sheathing ventilation (ASV) channel. Based on this conclusion and exploiting an existing mock-up facility, two equivalent pitched ventilated roofs with an air gap of 4 cm were built as coverage of two identical rooms, each one equipped with a fan coil, one with a 0.007-m PCM layer suspended in the middle of the ASV and the other one without. They were then tested under real conditions at the TekneHub Laboratory at the University of Ferrara. The behaviour of the two configurations were compared in terms of temperature, velocity of the air in the ASV, heat flux and energy requirement for cooling, which were monitored through T-type thermocouples, heat flow metre, anemometers and energy metres, respectively. The aim of the research was to validate the numerical results and confirm that the combination of the two strategies allows further improvement of roof performance.

Keywords: energy efficiency of buildings; ventilated roof; phase change materials; passive cooling

*Corresponding author: michele.bottarelli@unife.it

Received 25 November 2022; revised 13 March 2023; accepted 24 April 2023

1 INTRODUCTION

Accounting for 40% of the European Union's energy consumption, 36% of its CO_2 emissions and 55% of the electricity consumption, the building sector consistently affects the total global energy demand [1]. The ones responsible for this are heating and cooling systems [2], and with special regard to cooling, air conditioning is the main contributor to the peak electricity demand both in hot climates and during summer [3]. The continuously higher living standards together with the decrease of the cost of cooling equipment and the impact of the urban heat island effect, especially in crowded cities, are additional burdens to the actual scenario and will lead to further growth of energy requirement for HVAC systems, which is expected to increase by 80% until 2050, if compared to the 2010 levels [4].

Among the possible solutions to counteract this behaviour are passive cooling techniques, through which it is sometimes possible to improve building performance and indoor comfort without any additional energy demand. Song et al [5], among others, classified the main passive cooling methods identifying three main categories, namely, solar and heat control, heat exchange reduction and heat removal. Solar control is mainly done through shadings, which can be integrated within the buildings or made with vegetation. As regards heat exchange reduction, methods are

International Journal of Low-Carbon Technologies 2024, 19, 54–62

https://doi.org/10.1093/ijlct/ctad047 Advance Access publication 10 May 2023

divided between those without and those with thermal mass; the former consists of the addition of insulation layers, whereas the latter includes, for instance, the use of phase change materials (PCMs). PCMs have higher latent heat capacity and can absorb and release a larger amount of heat in a shorter temperature range around the phase change temperature when compared with sensible heat storage [6].

Heat removal can be achieved, for instance, through natural ventilation in ventilated roofs and facades. These are particularly effective in decreasing the heat transfer through the envelope, reducing the energy requirement for cooling, and turn out to be particularly effective in roofs, where heat transfer has been estimated to be around three times greater than the one through a south-facing facade [7]. In hot climates, such as in the Mediterranean, ventilated roofs allow the dissipation of the incoming heat during summer [8] and create an insulation layer around the building inner envelope in winter [9]. Their efficacy has been demonstrated by different experimental observations [10, 11]. In addition to this, the project LIFE Climate Change Adaptation HEROTILE (High Energy savings in building cooling by ROof TILEs shape optimization towards a better above sheathing ventilation [ASV]) [12] aimed at improving the performance of ventilated roofs by designing new tiles, namely, Marsigliese and Portoghese, that could improve the airflow through the tiles overlaps. The project consisted of numerical investigations and experimental activities, as documented in [13–15]. Further improvements on the performance of ventilated roofs might be obtained by the integration of PCM, as already proposed by some researchers. For instance, Kosny et al [16] carried out tests on an experimental ventilated roof in which the PCM was positioned under the fibreglass, below the air cavity, and obtained a reduction of 55% in the cooling load in summer. Hou et al [17] proposed a ventilated roof composed of multiple PCM, one positioned above the roof and the other one under the ventilation layer, above the indoor environment. They carried out different summer tests, obtaining a reduction of the peak indoor temperature up to 47% and an increase of the minimum indoor temperature between 19% and 40%. Yu et al. [18] numerically studied a 3D model of a ventilated roof in which, above the ventilation channel, a 0.03-m layer of form-stable PCM was embedded between two cement mortars and obtained a reduction of the peak indoor temperature of more than 4 K. Bottarelli et al. [19] carried out a numerical investigation about the integration of a layer of PCM inside the ventilation channel in two different positions, namely, one laid on the roof deck and the other one suspended in the middle of the air gap. They concluded that by allowing air to flow both above and below the PCM layer, a reduction of the energy load of about 18% can be obtained.

The research given here started from these conclusions drawn by Bottarelli et al. [19], who found that the complete charge and discharge of the PCM was more likely to occur with air flowing both above and below the PCM layer. Thus, this research consisted of arranging and monitoring two ventilated roofs, one used as a benchmark and the other in which a layer of PCM is suspended in the middle of the air channel. Plastic containers filled with inorganic salt with a melting temperature of 25°C [20] were put in the middle of a 0.04-m air channel. The behaviour of the two roof configurations was monitored in terms of temperature, heat flux and ASV velocity. Experimental results were in accordance with the numerical results previously obtained, since a reduction of about 15% of the heat load was measured. The experimental data were then used to calibrate a computational fluid dynamic (CFD) numerical model implemented in COMSOL Multiphysics v5.6 [21], which might be used afterwards to investigate the performance and help in the design of other ventilated roofs, by varying the ASV channel height, the PCM layer height or its thermal properties, i.e., melting and solidification temperature, relative ranges, etc.

2 METHODOLOGY

The research reported here was carried out in two steps. The first step consisted of a simultaneous and thorough experimental monitoring of two roof configurations (with and without PCM layer) and the analysis of the thermal and airflow data obtained. Then a CFD model of the roof configuration with the PCM layer was implemented in COMSOL Multiphysics, following the work of Bottarelli et al. [19]. This numerical model, whose results have been compared with experimental measurements, aims to be a first approach to the problem, and it is expected that its more sophisticated versions will allow new scenarios to be simulated with a suitable level of uncertainty.

2.1. Experimental mock-up

The experimental activity consisted of monitoring and further comparison of the performances of two equivalent ventilated roofs, one containing a layer of PCM and the other one not, which were arranged exploiting an existing mock-up facility located at the TekneHub Laboratory of the University of Ferrara. This mock-up building (Figure 1a) was originally constructed for the European project LIFE Climate Change Adaptation HEROTILE (High Energy savings in building cooling by ROof TILEs shape optimization towards a better ASV) and was partially modified for this research.

The mock-up has an 8×10 m^2 rectangular plan and is made of seven equivalent rooms, where five of them are the actual test rooms north–south oriented, and the two at the ends are guard rooms, used to ensure the same conditions in each of the test rooms. The structure is of steel and is cladded with sandwich panels for both exterior and interior walls. For what concerns the roof, which is 20° tilted with north–south-oriented pitches, the steel beams are covered by a 0.03-m wooden deck and a waterproof polyolefin membrane upon which the tiles supports were arranged. The two rooms set for the monitoring have both 0.04-m tiles supports, which formed the ASV, and the cladding layer made of Portoghese tiles. In one of the two roofs, a 0.007-m layer of PCM in the middle of the air cavity was arranged. The layer consisted of 0.30×0.30 m^2 plastic containers each filled

a) b)

Figure 1. *(a) Mock-up building at the TekneHub Laboratory at the University of Ferrara. (b) Arrangement of the PCM plastic containers in the ASV layer of the roof.*

in with about 0.42 kg of inorganic PCM with a melting point of about 25°C [20]. In Figure 1b, the arrangement of the PCM plastic containers is depicted. Several sensors were installed to monitor the behaviour of the two configurations. In terms of boundary conditions, a weather station was installed outside the laboratory and collected data about solar radiation, air temperature and humidity, wind speed and its direction every 15 minutes.

For more accurate measurements, additional sensors were installed, namely, a pyranometer parallel to the south pitch to measure the solar radiation, a RTD Pt100 outside the north wall to measure air temperature, and cup anemometers at different heights (1.50, 2.50, 4.00, 6.00 m) for the wind profile. For what concerns the monitoring of the two roof configurations, temperature and heat flux sensors together with hot wire anemometers were used. Their positions are shown in Figure 2a and b. T-type thermocouples (accuracy: 0.5 K) were installed on the tile intrados, in the middle of the ASV channel above and below the PCM layer, underneath one of the plastic containers, on the extrados and intrados of the wooden deck and inside the rooms. Each room has a fan coil unit to regulate indoor temperature, which was set to 26°C during the period of the test. The heat flux meter (accuracy: 3%) was installed on the intrados of the wooden deck next to the thermocouple, while two anemometers (operating range: 0.1–2.5 m/s, accuracy: 3% of reading +1% of full scale) were installed in the middle of the ASV channel, above and below the PCM layer. With respect to the roof without PCM, only one thermocouple and anemometer were positioned in the middle of the only ASV channel. In general, all the above-mentioned sensors were installed in the south-facing pitch and were connected to a data logger. Temperature and heat flux data were collected with a time step of 2 minutes, while wind speed data were collected every minute.

2.2. CFD model

In order to reduce computational cost, the CFD model reproduced a 2D section of the south pitch (Figure 3), including a 5 m × 8 m external environment. Due to the low thermal inertia of the system, 24 hours (10–11 May 2022) of simulation were selected among those of the experimental campaign in which the air conditioning system operated in cooling mode.

The Portoghese tiles of the covering were modelled as 0.41 m × 0.015 m rectangles, and the metal supports through which the ASV channel was built were modelled as a 1D screen layer to which a 70% of solidity, with an average hole dimension of 0.003 m, was assigned. The PCM plastic containers were modelled as 0.23 m × 0.007 m rectangles of PCM material surrounded by plastic rectangular frames (0.035 m × 0.007 m). The properties assigned to the different materials are given in Table 1. For what concerns the PCM density, a value of 1560 kg/m^3 was experimentally estimated during its liquid phase. However, since the default model length is of 1 m and the PCM layer is not a continuous layer but consists of separated plastic containers (four in a pitch width of 1.3 m), the density applied to the material was reduced proportionally in order to consider the same PCM mass as in the actual roof. Hence, the value assigned to the PCM material is 600 kg/m^3.

Regarding boundary conditions, indoor and outdoor temperatures and solar radiation were expressed as time-dependent functions according to the experimental data acquired (Figure 4). For what concerns the wind velocity profile assigned to the inlet of the fluid domain, the following power law (Equation 1) was used.

Wind speed profile:

$$v(z) = v_0\left(\frac{z}{z_0}\right)^{\alpha} \quad (1)$$

where

$v(z)$ = wind speed at height z (m/s)
z = height
v_0 = wind speed at a reference height, equal to 1 m/s
z_0 = reference height
α = empirical non-dimensional exponent, equal to 0.3 (masters)

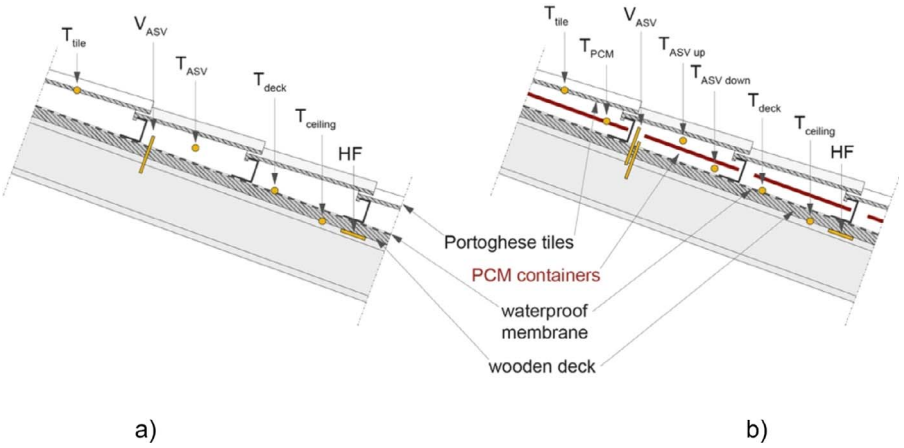

Figure 2. *Section of the roof configurations (a) without the PCM layer and (b) with the PCM layer.*

Table 1. *Physical properties of the building materials.*

Material	Thickness (m)	Density (kg/m^3)	Thermal conductivity (W/[m·K])	Specific heat (J/[kg·K])	Latent heat (kJ/kg)	Phase change temperature (°C)	Emissivity (−)
Tiles	0.015	1600	0.5	800	–	–	0.8
PCM	0.007	600∗	0.6	1800	100	24°C melting 23°C solidification (span 5°C)	0.94
Wooden deck	0.03	532	0.4	1000	–	–	0.9

∗The asterisk indicates what is explained in the manuscript, namely that the density indicated in the Table is not the effective density but rather an equivalent density, calculated according to the numerical model's properties.

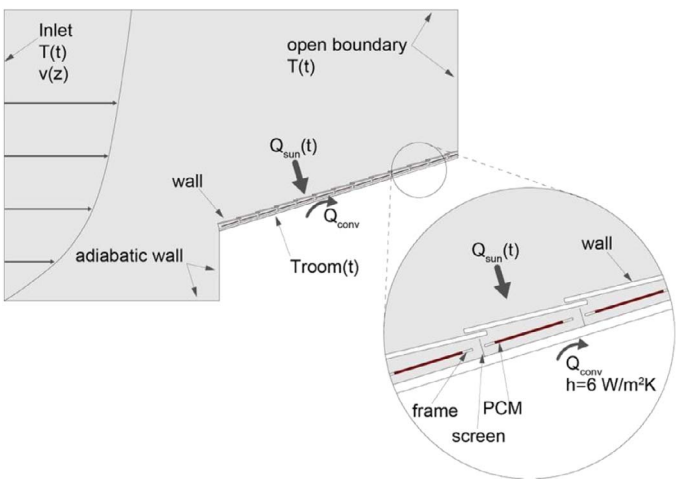

Figure 3. *Description of CFD domain and boundary conditions.*

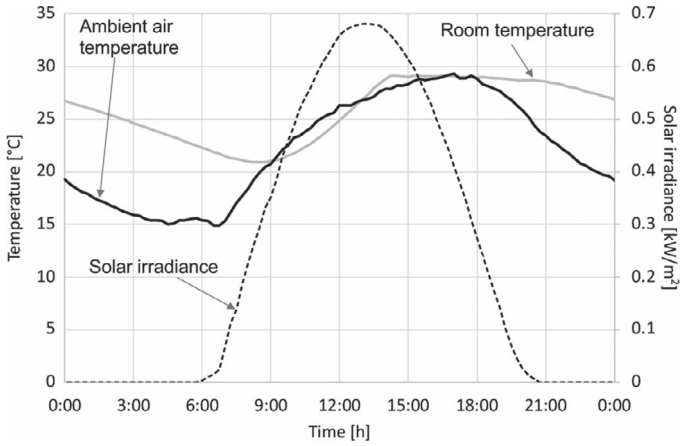

Figure 4. *Boundary conditions applied to the model.*

The k–ε model with standard wall functions was used to simulate turbulence within the fluid domain. The numerical problem was solved in two stages. First, a steady-state solution of the airflow was sought in the thermal conditions formerly described. Then, from the steady-state airflow solution, the heat transfer transient problem was solved. A relative tolerance of 10^{-3} was set for residuals. Meshes were locally refined in areas with high temperature and velocity gradients. After an independence grid study in which temperatures and air flow velocities were analysed, an unstructured mesh made of 48 127 elements was used, which showed an average element quality of 0.79. The grid independence was carried out, as depicted in Figure 5.

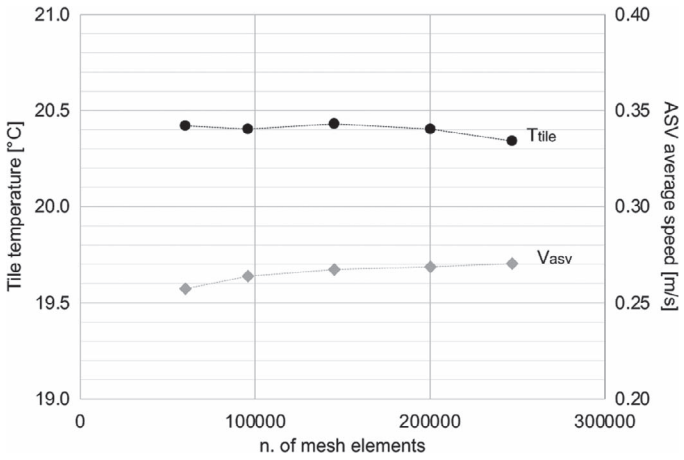

Figure 5. *Mesh independence study carried out.*

3 EXPERIMENTAL RESULTS

The roofs were arranged at the beginning of March 2022, and the monitoring activity has been carried out since. A period of five consecutive days (from 10 to 14 May 2022), with similar ambient conditions, was chosen for the purpose of this article, and the results are presented here. As regards the indoor conditions, the fan coil unit operated in cooling mode when indoor temperature exceeded the set point of 26°C. Outdoor air temperature and solar irradiance are reported in Figure 6a and wind speed and direction in Figure 6b. Air temperature fluctuated from a minimum of 12–15°C during the night up to almost 30°C during the day, with a horizontal solar irradiance that reached peaks of nearly 900 W/m^2. As for the wind, the velocity was around 1 m/s during the first and the last days, while for the rest of the days, it was slightly higher (between 1.5 and 2 m/s). The prevalent wind directions were south and west. From the comparison of the two roof configurations, the effect of the PCM is clearly visible. Temperatures inside the ASV are depicted in Figure 7a. During the day, the temperature within the ASV channel in the roof with PCM above the PCM layer (Tasv-up) was almost the same as that in the roof without PCM, while the temperature under the PCM (Tasv-down) was lower, with differences of about 5°C during the hottest hours of the day and which reached peaks up to 7°C during the morning when, based on the external conditions, the PCM was melting. On the contrary, during nighttime, both (up and down) ASV temperatures in the roof with PCM were higher than the ASV temperature on the roof without, with differences up to 5°C between midnight and 3 am. Again, this is likely due to the effect of the solidification of the PCM, which can be seen in the graph (Figure 7a) as sharp temperature changes around 25°C.

A similar behaviour can be observed on deck temperatures, depicted in Figure 7b, where during the day the deck temperature of the roof with PCM was up to 3°C lower than that of the roof without PCM, while during the night it was up to 2°C higher, in correspondence with the phase change of the PCM. Furthermore, and according to Fisher's *F*-test for comparing variances, temperature fluctuations at deck in the roof with PCM were significantly smaller than those in the roof without PCM, which agrees with the results of a previous CFD numerical study of this kind of roof configurations [19]. The standard deviation of deck temperature for the roof with PCM was 19% smaller than for the roof without. Thus, a slower degradation of the outer surface of the insulation layer caused by extreme temperatures is expected in the roof with PCM. There were no significant statistical differences between the average values according to *z*-test. For what concerns heat fluxes (Figure 7b), outgoing (positive) heat fluxes are measured mainly during night time, remaining nearly constant most of the time (4 W/m^2 on average, approximately), starting about 2 hours after sunset and vanishing about 3 hours after sunrise. The roof with PCM showed a smaller variance (*F*-test) but a statistically greater average (just 0.4 W/m^2, *z*-test) of these outgoing heat fluxes than the roof without PCM. Incoming (negative) heat fluxes took place 3 hours after sunrise and 2 hours before sunset, with peak values of around 35 and 31 W/m^2 for the roofs without and with PCM, respectively. In Figure 8, a detailed view of the heat flux through the roofs is depicted for one of the five days considered, more specifically 14 May. It was observed how peak values of incoming heat fluxes through the roof with PCM showed a delay of about 20 to 30 minutes with respect to the roof without PCM. Again, variances of these incoming fluxes were significantly smaller for the roof with PCM (*F*-test), showing a smaller average value as well (−10%, *z*-test). The addition of the PCM layer resulted in a reduction of about 5 W/m^2 in the hottest hours of the day, which corresponds to about 15% of the incoming flux through the roof without PCM.

The total incoming energy during the 5 days considered was calculated from the incoming heat flux and is shown in Figure 9a. In the case with PCM, there was about 8% less incoming energy through the roof, which means lower energy demand for cooling in the room. Regarding room temperature, during the day, the rooms had the same indoor temperature, which was kept constant with the help of fan coils. However, during the night, when the temperature was lower than the set point temperature and therefore the fan coil units were off, the presence of the PCM layer kept the room warmer, with temperature increases that reached almost 2°C.

The velocity of air inside the ASV is depicted in Figure 9b. In case of a roof without PCM, the velocity of the ASV was almost the same as that of the other roof under the PCM containers, with values that were lower than 0.1 m/s on average except for some peaks during the second and third days that reached 0.2 m/s. The velocity of air inside the ASV above the PCM containers was completely different, more than double than the one under the PCM containers on average and with peaks higher than 0.4 m/s. However, it has to be noticed that, in general, these air velocities are all quite low since Ferrara is characterised by frequent low wind speeds.

From the experimental measurements for a longer period (3 May to 16 June 2022), a multiple regression model (MLR) has been carried out (Equation 2) in order to estimate heat flux

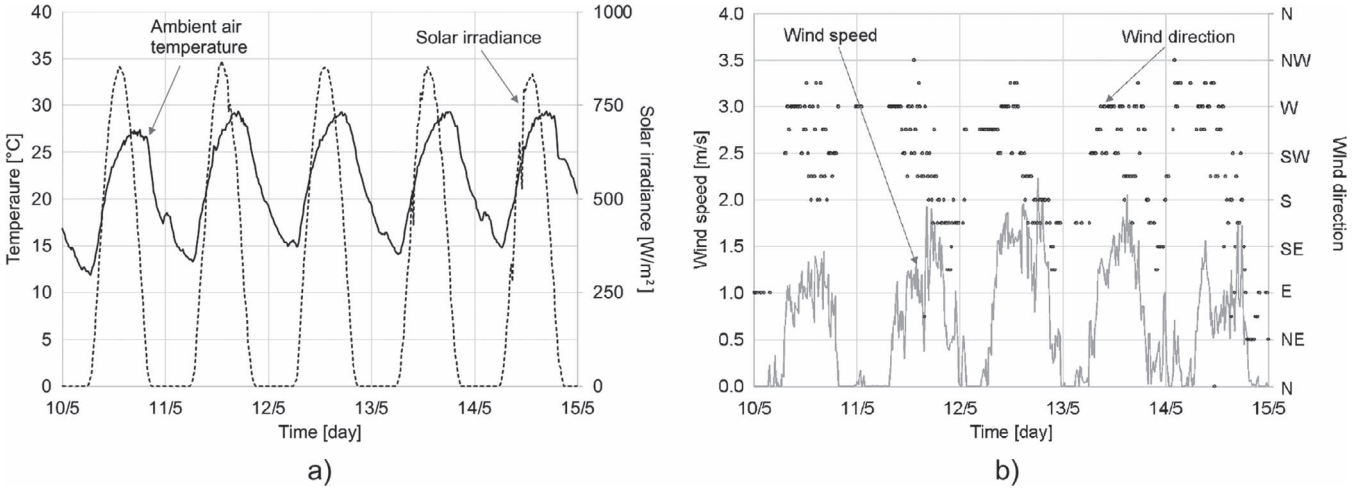

Figure 6. *Fifteen-minute average ambient conditions during the monitoring activity: (a) air temperature and solar radiation; (b) wind speed and direction.*

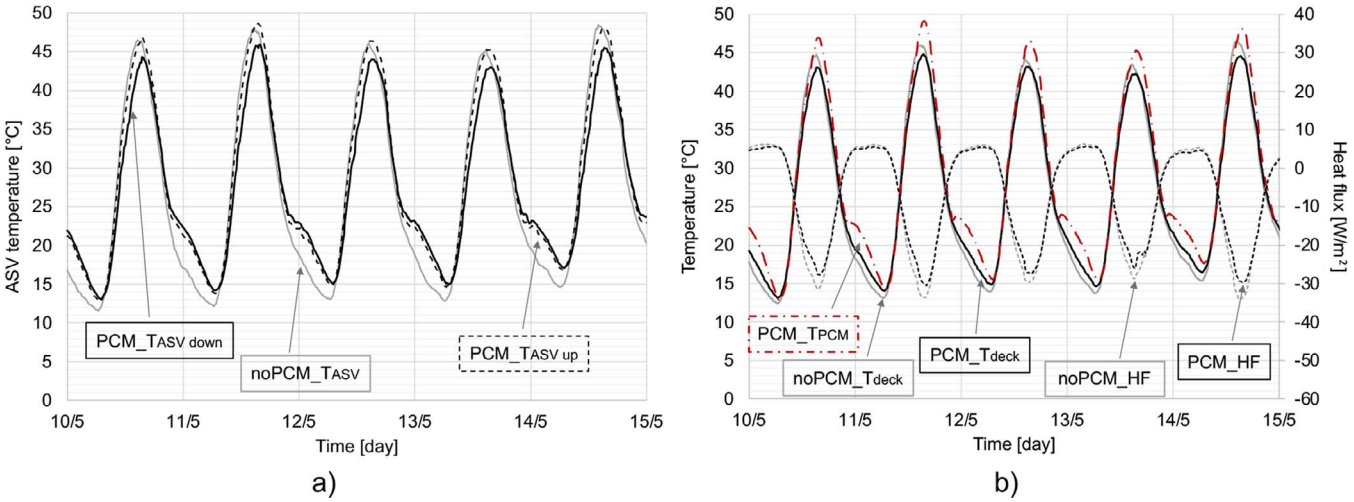

Figure 7. *Fifteen-minute average of (a) ASV temperature and (b) deck temperatures and heat fluxes of both the roof configurations monitored.*

Table 2. *Values of MLR model parameters (3 May to 16 June 2022).*

MLR model parameter	No PCM	PCM
β_0	2 592 948	2 453 770
β_1	−125 896	−121 624
β_2	−0.01843	−0.01459
R^2	0.824	0.820

through the roof (for both configurations), under cooling mode operation of fan coil unit, in terms of outdoor air temperature (T_{out}) and solar radiation (SR). Table 2 shows the parameters of the MLR model. The fitting can be considered statistically good (R^2 around 0.82 for both cases).

Multiple linear regression model:

$$HF = \beta 0 + \beta 1 \cdot Tout + \beta 2 \cdot I \quad (2)$$

where

HF = heat flux (W/m²)

T_{out} = outdoor ambient temperature (°C)

I = solar irradiance (W/m²)

In order to highlight the actual effect of PCM on the performance of the roofs, only data collected in the range between midday and 3 pm were considered in a second analysis, since ambient conditions are the most critical at that period. As reported in Table 3, during the selected 5 days, the average air temperature, solar radiation and wind speed were about 27.3°C, 820 W/m², and 1.3 m/s, respectively. Under these conditions, the differences already observed on deck and ASV temperatures are emphasised. Regarding the deck, the average temperature in the roof without PCM was 42.3°C, while that in the roof with PCM was 2.2°C lower, with a corresponding reduction of 5.2%. A greater reduction is visible in terms of ASV temperature, where the average in the roof without PCM was 44.5°C while in the roof with

Table 3. *Average data during the selected period in the range 12 to 3 pm.*

	Air temperature (°C)	Solar irradiance (W/m²)	Wind speed (m/s)	T_{tile} (°C)	T_{ASV} (°C)	T_{deck} (°C)	$T_{ceiling}$ (°C)	T_{room} (°C)	Heat gain (Wh/m²)
no PCM	27.3	820.2	1.3	52.6	44.5	42.3	28.9	24.9	77.0
PCM				52.2	39.4	40.1	29.2	25.1	65.4
Difference	–	–	–	−0.9%	−11.4%	−5.2%	+1.1%	+0.8%	−15.1%

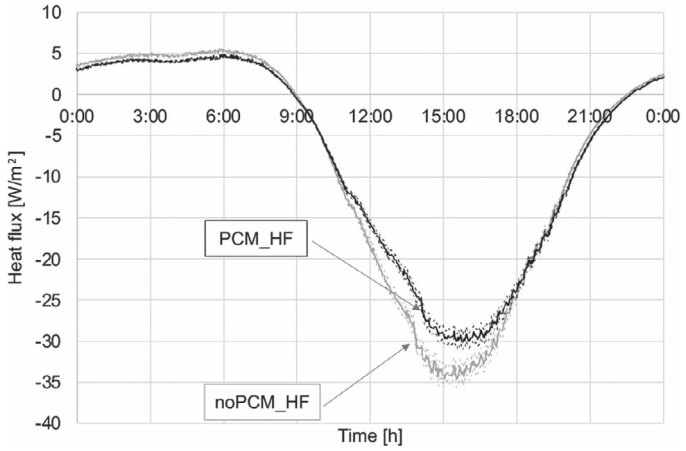

Figure 8. *Detail of the heat fluxes on 14 May. Ranges of experimental uncertainty are shown with dashed lines. Raw data were acquired with a time step of 2 min.*

PCM, under the PCM containers, was 39.4°C, corresponding to a reduction of 11.4%. The temperature of the tile was almost the same in the two configurations, with differences lower than 0.5°C. The same behaviour can be observed in the temperatures of the ceiling and the room, where the differences between the two configurations were lower than sensor uncertainty. Eventually, the incoming energy through the roof with PCM was 15.1% smaller than that through the roof without PCM, with an average daily difference of 11.6 Wh/m² during the hottest hours of the day and nearly 20 Wh/m² when considering the whole day.

4 NUMERICAL RESULTS

Comparisons between numerical and experimental results have been focused especially on thermal variables (temperature and heat flux) during the 5 days of monitoring activity, and results are reported in Figure 10a and b. Thus, as for the temperatures inside the ASV channel, the differences between the experimental and the simulated data are of about 0.6°C on average. More specifically, if compared with the experimental values, during the night and between 3 pm and 6 pm, the simulated values are about 1°C lower, while during the morning and after sunset, they are from 2°C to 4°C higher. For what concerns the temperature of the PCM tile, the average difference between the experimental and simulated values is about 1.5°C (simulated values are about 2°C and 5°C higher during nighttime and daytime, respectively). As for the deck temperature, the difference between the experimental and the simulated values is almost constant, with simulated values always between 2°C and 3°C higher than the experimental ones. Regarding the heat flux, the average difference between the experimental and simulated values is 0.2 W/m², with simulated values lower than the experimental ones during the morning and after 3 pm while higher between 9 am and 1 pm. The root mean square errors (RMSE) were also estimated, and values are reported in Table 4. Regarding temperatures, RMSE values range between three and five times the experimental uncertainty, with lower values for the temperatures inside the ASV channel, while as for the heat flux, the RMSE value is between two and three times the experimental uncertainty, showing a good agreement between the experimental and the numerical results.

5 CONCLUSIONS

The total global energy demand is strongly affected by the building sector, especially because of the energy required for heating and cooling in buildings. With special regards to cooling, the global demand is expected to drastically increase over the coming decades. The adoption of passive cooling strategies might be useful to tackle this issue by reducing the energy demand for cooling through the improvement of the building design and its envelope. This can be achieved through solar control, which can be done with shadings, heat removal, feasible with ventilated facades and roofs, or heat exchange reduction, using for instance insulation layers or PCMs. The former has become one of the most widely used strategies to reduce the heat exchange though the envelope and has hence become relatively cheap. However, the reduced heat exchange that prevents during the day part of the heat from entering into the building also prevents during the night the dissipation of the heat entered. This phenomenon might lead to the overheating of the building, which can worsen the quality of the indoor environment.

Focus of this research was the experimental monitoring of a real-scale application of two of the above-mentioned solutions, namely, a ventilated roof and the use of PCMs, which were combined together. Both the strategies considered have already individually proven to be effective in improving the energy performance of buildings; hence, this research aimed at evaluating whether the combination brought further improvements.

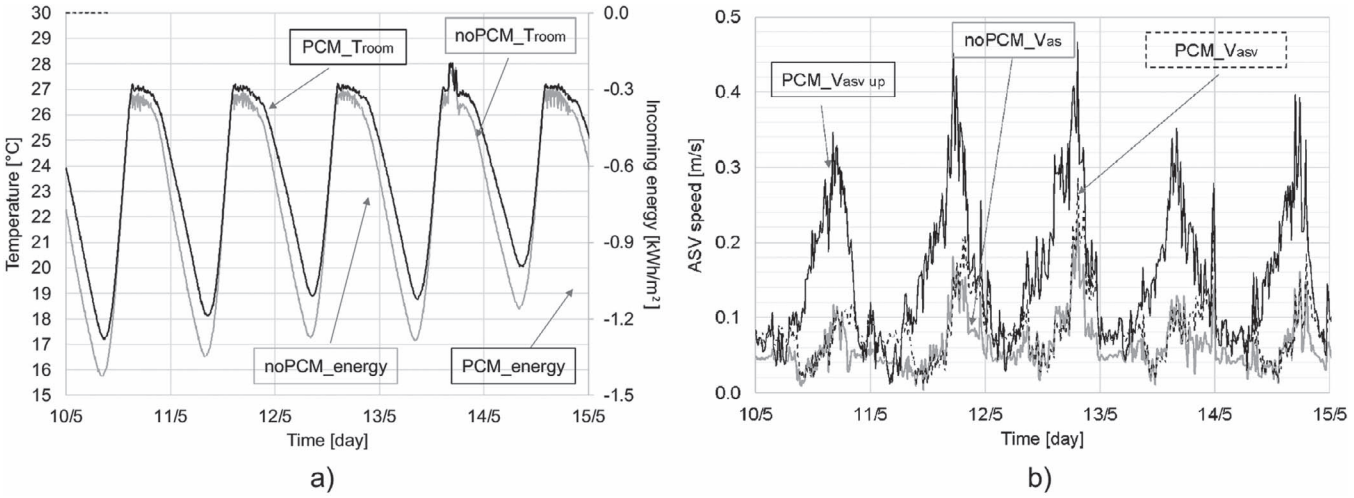

Figure 9. *Fifteen-minute average of (a) room temperature and total heat gain from the roof; (b) air velocity in the ASV.*

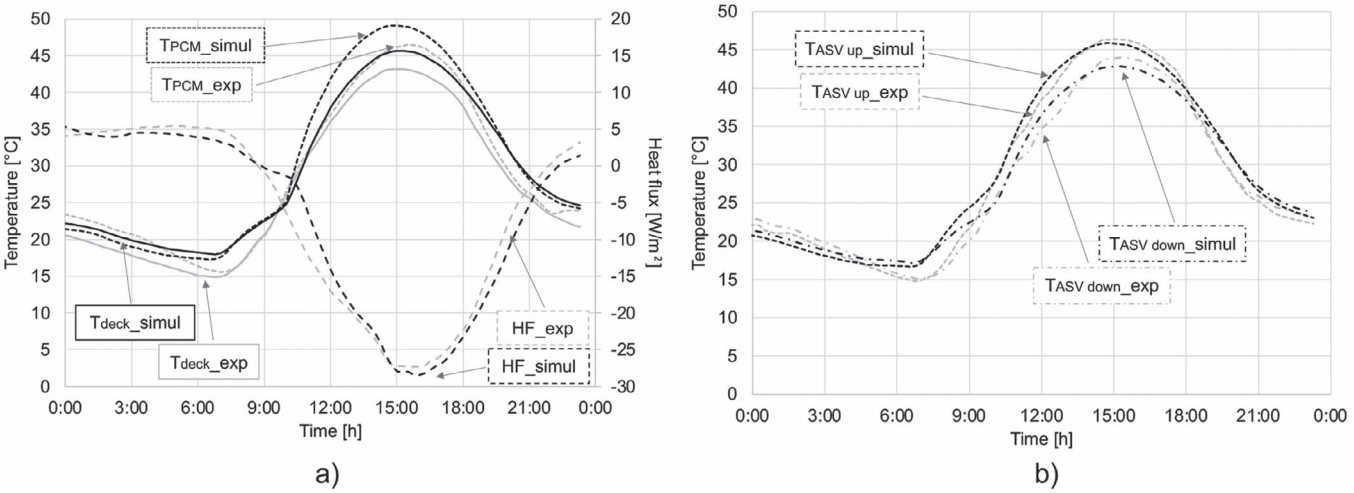

Figure 10. *Simulated and experimental values of (a) ASV temperatures and (b) PCM and deck temperatures and heat flux (12 May 2022).*

Table 4. *RMSE values of CFD simulated data.*

	T_{PCM} (°C)	$T_{ASV\ up}$ (°C)	$T_{ASV\ down}$ (°C)	T_{deck} (°C)	Heat flux (W/m^2)
RMSE	2.52	1.53	1.56	2.55	2.16

An experimental activity was carried out at the TekneHub Laboratory at the University of Ferrara where two equivalent ventilated roofs were arranged, one with a layer of PCM suspended in the middle of the air channel and the other one without PCM layer. The layer of PCM consisted of an inorganic PCM with a melting temperature of about 24–25°C and contained in plastic containers. The roofs were constantly monitored since March 2022. The experimental results confirmed the effect of the PCM layer in reducing the peak temperatures as well as reducing the incoming heat fluxes. In fact, the addition of PCM inside the ASV channel brought a reduction of the maximum temperature up to 5°C during the hottest hours of the day, corresponding to a reduction of 11.4%, while below the ASV channel and above the wooden deck, the maximum temperature reached was 2°C lower during the day, corresponding to a reduction of 5.2%. It was up to 3°C higher during the night. For what concerns the incoming energy, the PCM layer brought an average reduction of 8% considering the whole day and up to 15% during the hottest hours of the day. In terms of air velocity in the ASV channel, the velocity monitored below the PCM layer was the same as in the roof without PCM, while the velocity above the PCM layer was more than double. These velocities, however, were all quite

low due to the low wind speed. Moreover, from a closer look on the PCM plastic container, the maximum temperature reached was very high, which might mean an undersized PCM layer or a too low melting temperature. The experimental results were then used to validate a simplified 2D numerical model of the south pitch, which can be considered a good approach to the problem and a first step for the development of more advanced CFD models, which can be used for further investigations considering different boundary conditions, climatic zones, as well as changing the geometry and PCM thermal characteristics.

AUTHOR CONTRIBUTIONS

Michele Bottarelli: Conceptualization, Formal analysis, Investigation, Methodology, Software, Supervision, Validation, Writing — review and editing; Eleonora Baccega: Conceptualization, Data curation, Investigation, Methodology, Writing — original draft; Francisco Javier Gonzalez Gallero: Data curation, Formal analysis, Investigation, Methodology, Writing - review and editing; Ismael Rodriguez Maestre: Supervision, Validation, Writing — review and editing; Gang Pei: Formal Analysis, Supervision, Validation, Writing — review and editing; Yuehong Su: Formal Analysis, Supervision, Validation, Writing — review and editing

DATA AVAILABILITY STATEMENT

The data underlying this article will be shared on reasonable request to the corresponding author.

ACKNOWLEDGEMENTS

The experimental activities reported here were possible thanks to the European project LIFE Climate Change Adaptation HEROTILE (High Energy savings in building cooling by ROof TILEs shape optimization towards a better ASV—LIFE14CCA/IT/000939), during which the mock-up facility was built.

REFERENCES

[1] European Parliament. *Boosting Building Renovation*, 2016. https://www.europarl.europa.eu/RegData/etudes/STUD/2016/587326/IPOL_STU(2016)587326_EN.pdf (27 March 2022, date last accessed).

[2] IEA, 2019. IEA website. https://www.iea.org/topics/energy-efficiency (18 November 2022, date last accessed).

[3] Chan HY, Riffat SB, Zhu J. Review of passive solar heating and cooling technologies. *Renew Sustain Energy Rev* 2010;**14**:781–9. https://doi.org/10.1016/j.rser.2009.10.030.

[4] Ürge-Vorsatz D, Cabeza LF, Serrano S *et al.* Heating and cooling energy trends and drivers in buildings. *Renew Sustain Energy Rev* 2015;**41**:85–98. https://doi.org/10.1016/j.rser.2014.08.039.

[5] Song Y, Darani KS, Khdair AI *et al.* A review on conventional passive cooling methods applicable to arid and warm climates considering economic cost and efficiency analysis in resource-based cities. *Energy Rep* 2021;**7**:2784–820. https://doi.org/10.1016/j.egyr.2021.04.056.

[6] Lizana J, Chacartegui R, Barrios-Padura A, Valverde JM. Advances in thermal energy storage materials and their applications towards zero energy buildings: a critical review. *Appl Energy* 2017;**203**:219–39. https://doi.org/10.1016/j.apenergy.2017.06.008.

[7] Chang P, Chiang C, Lai C. Development and preliminary evaluation of double roof prototypes incorporating RBS (radiant barrier system). *Energ Buildings* 2008;**40**:140–7. https://doi.org/10.1016/j.enbuild.2007.01.021.

[8] Ciampi M, Leccese F, Tuoni G. Energy analysis of ventilated and microventilated roofs. *Sol Energy* 2005;**79**:183–92. https://doi.org/10.1016/j.solener.2004.08.014.

[9] Dimoudi A, Androutsopoulos A, Lykoudis S. Summer performance of a ventilated roof component. *Energ Buildings* 2006;**38**:610–7. https://doi.org/10.1016/j.enbuild.2005.09.006.

[10] Lee S, Park SH, Yeo MS, Kim KW. An experimental study on airflow in the cavity of a ventilated roof. *Build Environ* 2009;**44**:1431–9. https://doi.org/10.1016/j.buildenv.2008.09.009.

[11] Baccega E, Bortoloni M, Bottarelli M *et al.* Improving the air permeability of ventilated roofs. *Future Cities Environ* 2022;**8**:1–8.

[12] HEROTILE. *Life Herotile Website*. https://www.lifeherotile.eu/it/ (18 November 2022, date last accessed).

[13] Bottarelli M, Bortoloni M, Dino G. Experimental analysis of an innovative tile covering for ventilated pitched roofs. *Int J Low Carbon Tech* 2018;**13**:6–14. https://doi.org/10.1093/ijlct/ctx014.

[14] Bottarelli M, Bortoloni M, Zannoni G *et al.* CFD analysis of roof tile coverings. *Energy* 2017a;**137**:391–8. https://doi.org/10.1016/j.energy.2017.03.081.

[15] Bottarelli M, Bortoloni M. On the heat transfer through roof tile coverings. *Int J Heat Tech* 2017b;**35**:S316–21. https://doi.org/10.18280/ijht.35Sp0143.

[16] Kosny J, Biswas K, Miller W, Kriner S. Field thermal performance of naturally ventilated solar roof with PCM heat sink. *Sol Energy* 2012;**86**:2504–14. https://doi.org/10.1016/j.solener.2012.05.020.

[17] Hou M, Kong X, Li H *et al.* Experimental study on the thermal performance of composite phase change ventilated roof. *J Energy Storage* 2021;**33**:102060. https://doi.org/10.1016/j.est.2020.102060.

[18] Yu J, Leng K, Wang F *et al.* Simulation study on dynamic thermal performance of a new ventilated roof with form stable PCM in southern China. *Sustainability* 2020;**12**:9315. https://doi.org/10.3390/su12229315.

[19] Bottarelli M, González Gallero JF, Rodríguez Maestre I *et al.* Solar gain mitigation in ventilated tiled roofs by using phase change materials. *Int J Low Carbon Tech* 2020;**15**:434–42. https://doi.org/10.1093/ijlct/ctaa001.

[20] Templok. https://e-4epcm.it/product/templok/ (11 March 2023, date last accessed).

[21] COMSOL *Multiphysics Reference Manual*. http://www.comsol.com (19 November 2020, date last accessed).